Sinusoidal Efflux of Taurocholate Is Enhanced in Mrp2-Deficient Rat Liver[1]

Hidetaka Akita,[2] Hiroshi Suzuki,[2] and Yuichi Sugiyama[2,3]

Received April 1, 2001; accepted May 6, 2001

Purpose. It has been shown that plasma concentration and urinary excretion of bile acids is elevated under the cholestatic/hyperbilirubinemic conditions. Previously, it was demonstrated that the plasma concentration of bile acids was elevated in the multidrug resistance-associated protein 2 (Mrp2)-deficient rats. The purpose of the present study was to compare the sinusoidal efflux clearance of taurocholate (TC) between Mrp2-deficient Eisai hyperbilirubinemic rats (EHBR) and normal rats.

Method. Hepatic disposition of the [^{3}H]TC was examined in the perfused liver. Apparent efflux clearance ($PS_{net,\ eff}$) of [^{3}H]TC from hepatocytes to outflow across the sinusoidal membrane was defined as the amount of [^{3}H]TC excreted into the outflow from the liver divided by hepatic AUC of [^{3}H]TC. Additionally, influx clearance (PS_{inf}) was also determined by multiple indicator dilution method because $PS_{net,\ eff}$ is also affected by PS_{inf}.

Results. $PS_{net,\ eff}$ was significantly higher in EHBR than that in Sprague–Dawley (SD) rats (16.6 ±1.7 vs. 6.1 ± 1.3 μL/min/g liver, $P < 0.01$). In contrast, PS_{inf} was comparable between SD rats and EHBR. Kinetic analysis suggested that the intrinsic clearance for the efflux of [^{3}H]TC across the sinusoidal membrane in EHBR was higher than that in SD rats (10.4 ± 1.0 v.s. 23.3 ± 1.7 μL/min/g liver, $P < 0.01$).

Conclusions. Enhanced sinusoidal efflux of TC in EHBR may be related to the altered disposition of bile acids in the mutant rats. Because Mrp3 transports TC and its expression is induced on the basolateral membrane of Mrp2-deficient rats, the enhanced sinusoidal efflux of TC in EHBR may be accounted for, at least partially, by the increased expression of Mrp3.

KEY WORDS: multidrug resistance-associated protein; Mrp3; sinusoidal efflux; perfused liver; taurocholate.

INTRODUCTION

Previous studies have shown that plasma concentration and urinary excretion of bile acids is elevated under cholestatic/hyperbilirubinemic conditions. Indeed, it has been demonstrated that the plasma concentration and urinary excretion of bile acids in cholestatic patients are higher than those in healthy subjects (1). Similarly, in rat models used to study the pathology of extrahepatic cholestasis (bile duct ligation-treated rats), an increase in the urinary excretion and the plasma concentration of bile acids also has been observed (2). Moreover, in the multidrug resistance-associated protein 2 (Mrp2)-deficient rats [e.g., Eisai hyperbilirubinemic rats (EHBR) (3) and TR^- rats (4)], a significant increase in plasma concentration of bile acids was observed. Because the liver is the major organ associating with the clearance of the bile acids from plasma under the pathologic conditions, these observations can be explained by the altered intrahepatic disposition of bile acids.

It has been shown that transporters located on the sinusoidal membrane and on the canalicular membrane are involved synergistically in the hepatic disposition of xenobiotics and bile acids. Recently, many kinds of transporters for the hepatobiliary excretion of bile acids have been identified (5–7). Concerning the sinusoidal transport, it has been established that transporters (such as Na^+-taurocholate cotransporting polypeptide (Ntcp) (8,9) and organic anion-transporting polypeptide (Oatp) (10–13) are involved in the uptake of bile acids from blood to the hepatocyte. Moreover, the transport of monovalent bile acids (such as taurocholate; TC) across the canalicular membrane is mediated by primary active transporter referred to as the bile salt export pump (Bsep) (14–16). Using membrane vesicles isolated from Sf9 cells infected with recombinant baculovirus containing cDNA for the sister of P-glycoprotein (Spgp), which was cloned as a homologue of MDR1 P-glycoprotein, it has been shown that this protein exhibits Bsep activity (14–16). In addition to these transporters, we and other researchers have reported previously that the expression of Mrp3 on the hepatic basolateral membrane is induced under cholestatic and/or Mrp2-deficient conditions (17–20). Because Mrp3 can efficiently excrete bile acids (TC, glycocholate, and taurolithocholate sulfate) (21,22), it is possible that Mrp3 is involved in the altered disposition of bile acids under these pathologic conditions. These previous observations suggest that variation of the hepatic disposition of bile acids is associated with the altered function of these transporters.

The purpose of this study was to compare the apparent sinusoidal efflux clearance ($PS_{net,\ eff}$) of TC, a major component of bile acid between normal rats and EHBR. Because $PS_{net,\ eff}$ is affected by the influx clearance (PS_{in}), PS_{in} was also determined by a multiple indicator dilution method.

MATERIALS AND METHODS

Materials

Unlabeled and [^{3}H]-labeled TC (2.0 μCi/nmol) were purchased from Sigma Chemical Co. (St Louis, MO) and New England Nuclear (Boston, MA), respectively.

[^{14}C]-labeled inulin (2.64 mCi/g) was purchased from New England Nuclear. Other chemicals used were available commercially and were reagent grade products. Male EHBR and Sprague–Dawley (SD) rats (7–8 weeks old) were purchased from Nihon SLC (Shizuoka, Japan). Rats were kept in SPF room until they were 10 weeks old and then used in the experiments. Polyclonal anti-rat Ntcp and Oatp-1 antibodies were supplied by Dr. Peter J Meier in Division of Clinical Pharmacology and Toxicology, Department of Medicine, University Hospital, Zurich (23,24). Antiserum for rat Bsep, raised in rabbits against an oligopeptide (the carboxyl termi-

[1] Part of this present study was presented at the 51st Annual Meeting of the American Association for the Study of Liver Disease, Dallas, Texas, October 27–31, 2000, appearing in abstract form in *Hepatology* **32**:428A (2000).

[2] Graduate School of Pharmaceutical Sciences, The University of Tokyo, Hongo, Bunkyo-ku, Toyko, 113-0033, Japan and CREST, Japan Science and Technology Corporation.

[3] To whom correspondence should be addressed. (e-mail: BXG05433@nifty.ne.jp)

nal of rat Bsep; AYYKLVITGAPIS) (14), was used in the present study. The polyclonal anti-rat MRP3 antibody, raised against a maltose-binding protein fusion protein containing the 136 amino acids corresponding to bases 838–973 of the deduced rat MRP3 amino acid sequence, was used in the present study (22).

Liver Perfusion Study

For the single-pass perfusion experiments, the liver was perfused by the method reported previously (25). After cannulation to the portal vein to allow infusion of the perfusate, and the hepatic venous vein to allow the outflow to be collected, the common bile duct was also cannulated to allow bile specimens to be collected. The perfusate consisted of 3 % bovine serum albumin in the Krebs–Ringer bicarbonate buffer (pH 7.4). Because the weight of the liver in EHBR was significantly higher than that in SD rats [15.6 ± 1.0 g vs. 10.1 ± 0.5 g, $P < 0.01$)], liver from EHBR was perfused at a higher flow rate (30–32 mL/min vs. 25–28 ml/min). Initially, 0.1 μM [^{3}H]TC was perfused continuously for 40 min to collect bile and outflow samples at 10-min intervals during this period. After this 40-min perfusion, the liver was then perfused with Krebs–Ringer bicarbonate buffer free of [^{3}H]TC for additional 30 min. During this washout period, bile was also collected for the intervals of 40–43 min, 43–50 min, 50–60 min, and 60–70 min. Outflow was collected at 20-s intervals during 40–43 min and collected further at intervals of 43–50 min, 50–60 min and 60–70 min. After a 30-min perfusion, the liver was excised to determine the remaining amount of [^{3}H]TC in the liver. The concentration of [^{3}H]TC in outflow and bile was measured in a liquid scintillation counter (LS 6000SE, Beckman Instruments, Fullerton, CA) after the addition of scintillation cocktail (Hyonic Flow®, Packard, Meriden, CT). To measure the amount of [^{3}H]TC associated with the liver, pieces of the liver (100–150 mg) were dissolved in Soluene-350 (Packard). The isotope concentration was determined in a liquid scintillation counter (LS 6000SE) after the addition of scintillation cocktail (Hyonic Flow®).

In the present study, multiple indicator dilution experiments were also performed. After the stabilization period of 10 min, 200 μL of the perfusion solution containing [^{14}C]inulin (0.03 μCi), an extracellular reference, and the test substance [^{3}H]TC (10 μCi) was injected as a bolus in the portal vein. After injection, the total effluent from the hepatic venous vein was collected at 1-s intervals for 17 s. The radioactivity from ^{14}C and [^{3}H] in the collected samples were determined in a liquid scintillation counter (LS 6000SE).

Data Analysis

The fraction of the infused amount excreted into bile and outflow were defined as follows:

$$\text{Fraction excreted into bile} = V_{bile}/I \quad (1)$$

$$\text{Fraction excreted into outflow} = V_{out}/I = C_{out}/C_{in} \quad (2)$$

where V_{bile} and V_{out} denote the excretion rate of [^{3}H]TC into the bile and the outflow, respectively, I represents the infusion rate of [^{3}H]TC, and C_{in} and C_{out} represent the concentration of [^{3}H]TC in the portal inflow and the hepatic venous outflow, respectively.

The liver concentration of [^{3}H]TC at indicated times was calculated with the sum of the amount of [^{3}H]TC remaining in the liver after 70-min perfusion and the cumulative excreted amount of [^{3}H]TC into the bile and the outflow from indicated time to 70 min. The area under the hepatic concentration-time curve (Hepatic AUC) of [^{3}H]TC from 40 min to 70 min (AUC_{liver}) was determined as the sum of the trapezoid area. Net permeability-surface area (PS) product of [^{3}H]TC from hepatocytes to outflow across the sinusoidal membrane ($PS_{net,\ eff}$) and PS product of [^{3}H]TC from liver to bile across the canalicular membrane (PS_{bile}) were calculated with the following equation:

$$PS_{net,eff} = X_{out}/AUC_{liver} \quad (3)$$

$$PS_{bile} = X_{bile}/AUC_{liver} \quad (4)$$

where X_{out} and X_{bile} denote the total amount of [^{3}H]TC recovered from the outflow and bile during 40–70 min, respectively.

In the present analysis, $PS_{net,\ eff}$ is given as a hybrid parameter, which is given by the following equation:

$$PS_{net,eff} = Q/(Q + CL_{int}) \quad (5)$$

where PS_{eff}, Q, and CL_{int} represent the intrinsic PS product of [^{3}H]TC from hepatocytes to outflow across the sinusoidal membrane, perfusate flow rate and biliary excretion clearance given by the following equations, respectively.

$$CL_{int} = PS_{inf} \cdot PS_{bile}/(PS_{eff} + PS_{bile}) \quad (6)$$

where PS_{inf} represents PS product for the hepatic uptake of [^{3}H]TC from perfusate to hepatocytes.

PS_{inf} was determined by the multiple dilution method reported previously (26). The natural logarithm of [^{14}C]inulin concentration to [^{3}H]TC concentration in the outflow was plotted as a function of time after correcting for the large vessel transit time. The initial slope of this plot, calculated by a linear regression analysis, reflects the influx rate constant (K_1). PS_{inf} can be calculated by the following equation:

$$PS_{inf} = K_1 \cdot V_{exp} \quad (7)$$

where V_{exp} represents the extracellular volume, which can be estimated by multiplying the perfusate flow rate by the transit time of the extracellular reference.

Using PS_{inf}, PS_{bile} and $PS_{net,\ eff}$ values calculated with equations 3, 4, and 7 , PS_{eff} value was calculated using Equations 5 and 6.

Statistical Method

The results are shown as mean ± SE. Student's *t*-test was used to determine the significance of differences between the two groups.

Crude Membrane Preparation

Crude membranes were prepared as described previously (18). Briefly, livers were homogenized in *buffer A* containing 250 mM sucrose, 1 mM EGTA, and 5 mM HEPES (pH 7.4) with a Dounce homogenizer. After centrifugation of the homogenate at 1,500 *g* for 15 min, the resulting pellet was suspended in *buffer A* and Percoll (Pharmacia Biotech, Uppsala, Sweden), and centrifuged at 30,000 *g* for 60 min. The turbid layer was suspended in *buffer B* containing 250 mM sucrose and 50 mM Tris · HCl (pH 7.4) and centrifuged at

8,000 *g* for 10 min. The resulting pellet was suspended in *buffer B,* homogenized with a Dounce homogenizer, and layered over 38% sucrose. After centrifugation at 16,000 *g* for 70 min, the interfaces were collected, washed by centrifugation at 75,000 *g* for 30 min in *buffer B,* and suspended in *buffer B* using a Teflon homogenizer. All procedures were performed at 0–4°C. The crude membrane was stored at −80°C before being used for western blot analysis.

Western Blot Analysis

Membrane proteins (10, 20, and 40 μg) were solubilized in a sample buffer consisting of 2 % SDS, 30 % glycerol, and 0.01 % bromophenol blue (pH = 6.8). The suspension was subjected to SDS-polyacrylamide gel electrophoresis (PAGE), electrotransferred to a polyvinyligene difluoride membrane (Millipore, Bedford, MA) using a blotter (Transblot; Bio-Rad, Richmond, CA) at 15 V for 1 h. The membranes were blocked with Tris-buffered saline containing 0.05% tween 20 (TBS-T) and 5% BSA 60 min at 4°C. Then, membranes were incubated with the following concentrations of primary antibodies in TBS-T containing 0.5% BSA overnight at 4°C and then washed with TBS-T (35min): polyclonal anti-rat Ntcp serum (dilution 1:5,000) (24), polyclonal anti-rat Oatp-1 serum (dilution 1:2,000) (23), polyclonal anti-rat Spgp antibody (1:1000) (14), and polyclonal anti-rat MRP3 antibody (1:2000) (22). The membranes were allowed to bind ^{125}I-labeled donkey anti-rabbit IgG antibody (dilution 1:200 in TBS-T containing 0.5 % BSA) for 1 h at room temperature, then were placed in contact with an imaging plate for 3 h after being washed with TBS-T (3 × 5 min). The intensity of specific bands was quantified by BAS 2000 system (Fuji Photo Film, Tokyo, Japan). The relative induction ratio was defined as the ratio of the intensity of a specific band in EHBR to that in SD rats.

RESULTS

Disposition of [^{3}H]TC in the Perfused Liver

In the present study, isolated livers from SD rat and EHBR were perfused with Krebs–Ringer bicarbonate buffer containing 0.1 μM [^{3}H]TC. The bile flow rate in SD rats and EHBR was maintained constant through the experiment (Fig. 1). The time profile for the excretion rate into bile and that into the outflow, along with the values normalized in term of the inflow rate, is shown in Figs. 2 and 3. At 40 min, V_{bile} / I in EHBR (0.75 ± 0.06) was significantly (P <0.05) lower than that in SD rats (0.96 ± 0.04). In contrast, V_{out} / I in EHBR (0.14 ± 0.02) was significantly (P <0.05) higher than that in SD rats (0.05 ± 0.01). The estimated hepatic concentration of [^{3}H]TC in EHBR (3.5 ± 0.4 μM) was not significantly different from that in SD rats (2.8 ± 0.3 μM) at 40 min.

Washout Experiments

In the washout experiments, V_{out} in EHBR was significantly higher than that in SD rats and total amount of [^{3}H]TC recovered from the outflow during 40 min to 70 min (X_{out}) in SD rats and EHBR was 205 ± 60 pmol/g liver and 756 ± 91 pmol/g liver, respectively. To determine the hepatic AUC, time profiles for hepatic concentration were determined (Fig. 4). The hepatic AUC values in SD rats and EHBR, calculated

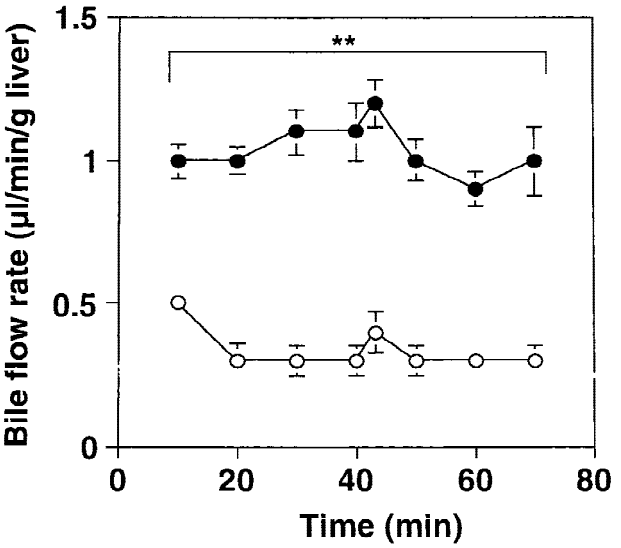

Fig. 1. Time profiles for the bile flow rate. Livers isolated from 10-week-old EHBR (○) and SD rats (●) were perfused as described in Materials and Methods. Each point and vertical bar represents the mean ± SE of n = 6 experiments. **Significantly different form SD rats (P <0.01).

from the time profiles of hepatic TC concentrations, were determined as 31.3 ± 4.4 μmol · min/L and 46.1 ± 3.2 μmol · min/L, respectively. Table I summarizes the calculated kinetics parameters. The $PS_{net,\ eff}$ in EHBR was approximately 2.5 times higher than that in SD rats (P <0.01; Table I). In contrast, PS_{bile} in EHBR was approximately 60% of that in SD rats (P <0.01; Table I). Consequently, the fraction of

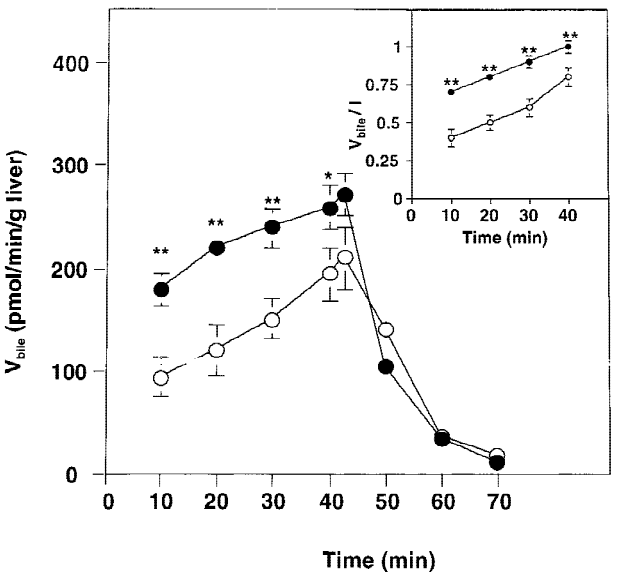

Fig. 2. Time profiles for the biliary excretion rate of taurocholate. Livers isolated from 10-week-old EHBR (○) and SD rats (●) were perfused with the medium containing [^{3}H]TC for the initial 40 min. At 40 min, the perfusate was changed to the medium free of [^{3}H]TC to examine the efflux of the preloaded isotope from the liver. Insert represents the biliary excretion rate divided by the infusion rate of [^{3}H]TC. Each point and vertical bar represents the mean ± SE of n = 6 experiments. *Significantly different form SD rats (P <0.05); **Significantly different form SD rats (P <0.01).

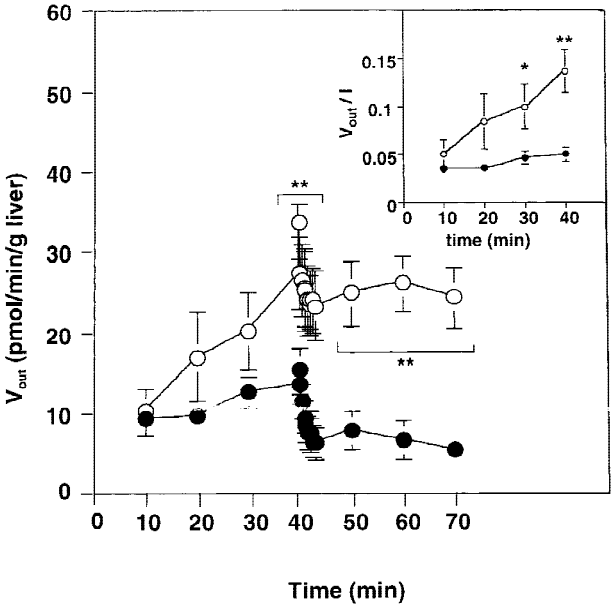

Fig. 3. Time profiles for the excretion rate of taurocholate into the outflow. Livers isolated from 10-week-old EHBR (■) and SD rats (●) were perfused with the medium containing [^{3}H]TC for the initial 40 min. At 40 min, the perfusate was changed to the medium free of [^{3}H]TC to examine the efflux of the preloaded isotope from the liver. Insert represents the excretion rate into the outflow divided by the infusion rate of [^{3}H]TC. Each point and vertical bar represents the mean ± SE of n = 6 experiments. **Significantly different form SD rats (P <0.01).

[^{3}H]TC excreted into the outflow in EHBR was 3.3 times higher than that in SD rats (P <0.01; Table I). In addition, the significantly lower ratio of X_{bile} to X_{total} in EHBR compared to SD rats was observed (P <0.01; Table I).

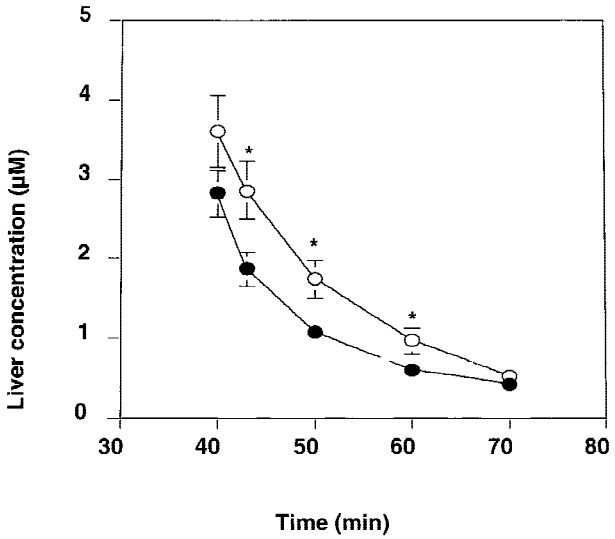

Fig. 4. Time profiles for the liver concentration of taurocholate. Hepatic concentration of EHBR (○) and SD rats(●) was calculated as the sum of the amount of [^{3}H]TC remaining in the liver at the end of the experiments (70 min) , and the cumulative excreted amount of [^{3}H]TC into the bile and the outflow from the indicated times to 70 min. Each point and vertical bar represents the mean ± SE of n = 6 experiments.*Significantly different form SD rats (P <0.05).

Table I. Kinetic Parameters for Taurocholate Determined in the Washout Experiment[a]

	SD	EHBR
$F_{outflow}$ (%)	8.3 ± 1.7	27.5 ± 2.9[b]
F_{bile} (%)	91.6 ± 1.7	72.5 ± 2.9[b]
$PS_{net,eff}$ (μl/min/g liver)	6.1 ± 1.3	16.6 ± 1.7[b]
PS_{bile} (μl/min/g liver)	67.3 ± 5.0	40.0 ± 4.0[b]
PS_{inf} (ml/min/g liver)	11.5 ± 1.3	10.4 ± 0.7
PS_{eff} (μl/min/g liver)	10.4 ± 1.0	23.3 ± 1.7[b]

[a] Kinetic analysis was performed to calculate $PS_{net,eff}$ and PS_{bile} from the data shown in Figs. 2, 3, and 4. $PS_{net,eff}$ and PS_{Bile} were defined as the amount of [^{3}H]TC excreted into the outflow and the bile, divided by the hepatic AUC, respectively (equation 3 and 4). Detailed analysis methods are described in the text. This table also shows the fractions of preloaded [^{3}H]TC excreted into the outflow (F_{out}) and the bile (F_{bile}), which were defined as X_{out} and X_{bile} divided by the amount of [^{3}H]TC in the liver at the initiation of the washout experiment (40 min), respectively. PS_{inf} was determined by multiple indicator dilution method (Figure 5). PS_{eff} was calculated by equation 5 and 6 described in material and method.

[b] significantly different from SD rats ($p < .01$).

Multiple Indicator Dilution Experiments

Because $PS_{net,\,eff}$ is given as a function of PS_{inf} as represented as equation 5 and 6, PS_{inf} was compared between SD rats and EHBR by multiple indicator dilution method. The natural logarithm of the ratio of the outflow fractions of [^{3}H]TC and [^{14}C]inulin (ratio plot) in SD rats and EHBR is given as a function of time as shown in Fig. 5. The initial slope of the ratio plot remained linear over initial 7 s, and the slope was comparable between SD rats and EHBR. PS_{inf} values determined from the ratio plot along with the calculated PS_{eff}

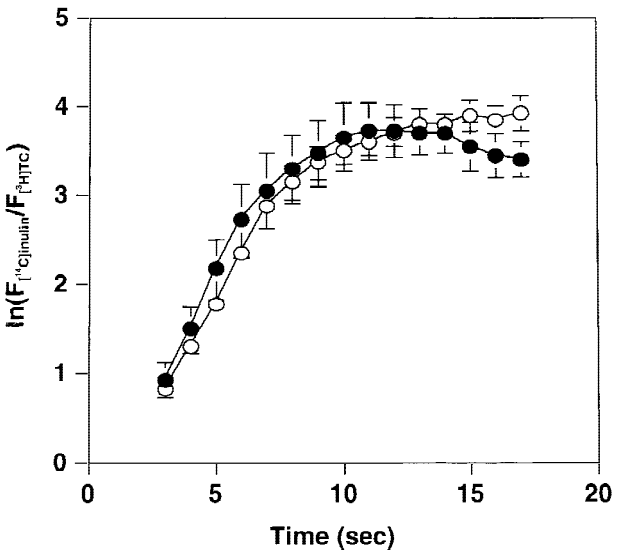

Fig. 5. Time profiles of the natural logarithm of the concenteration ratio of [^{14}C]inulin to [^{3}H]TC in the outflow. After the stabilization period of 10 min, 200 μL of the perfusion solution containing [^{14}C]inulin (0.03 μCi), an extracellular reference, and the test substance [^{3}H]TC (10 μCi) was injected as a bolus in the portal vein. After injection, the total effluent from the hepatic venous vein was collected at 1-s intervals for 17 s. ○ and ● represent SD rats and EHBR, respectively. Each point and vertical bar represents the mean ± SE of n = 3 experiments.

values are summarized in Table I. PS_{inf} values were comparable between SD rats and EHBR, and PS_{eff} in EHBR was 2.3 times higher than that in SD rats.

Hepatic Expression of Transporters

To discuss on the difference in the kinetics parameters between SD rats and EHBR in relation to the exression level of transporters, western blot was performed. As shown in Fig. 6, expression levels of the uptake transporters on the sinusoidal membrane (Ntcp and Oatp-1), and efflux transporter on the canalicular membrane (Spgp) and on the sinusoidal membrane (Mrp3) were quantified by western blot analysis. Antibodies recognized the band of 30 kDa, 80 kDa, 170 kDa, and 180 kDa for Ntcp, Oatp-1, Spgp, and Mrp3, respectively. Densitrometrical analysis showed that the ratio of the expression level of Ntcp and Oatp-1 and Spgp in EHBR to that in SD rat was 1.21 ± 0.1, 0.91 ± 0.1, and 1.22 ±0.2, respectively. Expression of Mrp3 was observed only in EHBR.

DISCUSSION

In the present study, we compared the sinusoidal efflux of TC from hepatocytes to blood between SD rats and EHBR in the perfused liver. Throughout the experiments, bile flow rate in EHBR was lower than that in SD rats, which is consistent with the previous observations (3). The kinetic analysis of the washout experiments showed that $PS_{net,\ eff}$ in EHBR was 2.5 times higher than that in SD rats (Table I). In contrast to the increase in $PS_{net,\ eff}$ in EHBR, PS_{bile} in these mutant rats was approximately 60% of that in SD rats (Table I). As a consequence of these alterations in the PS products, the fraction of [^{3}H]TC excreted into the outflow was significantly higher in EHBR than that in SD rats (Table I). The reduction of PS_{bile} in EHBR may be accounted for by assuming the reduced function of the bile acid transporter on the canalicular membrane (Bsep) (14,15). However, because hepatic expression of Spgp was comparable between SD rats and EHBR (Fig. 6), the mechanism for the reduced PS_{bile} in EHBR compared to SD rats remains to be elucidated.

The increase in $PS_{net,\ eff}$ and the decrease in PS_{bile} in EHBR compared with SD rats may contribute to the altered disposition of bile acids in the mutant rats. In our experiments, at 40 min after initiation of the infusion of [^{3}H]TC, the fraction of infused [^{3}H]TC excreted into bile in SD rats was 0.96 ±0.04, whereas the corresponding value was 0.75 ± 0.06 in EHBR. Such an alternation in TC disposition has also been observed in the previous in vivo studies using Mrp2-deficient rats. Jansen *et al.* (27) injected TC to normal Wistar rats and Mrp2-deficient TR$^-$ rats to determine the time profiles for the plasma concentration and the cumulative amount excreted into bile. As far as the plasma disappearance curve was concerned, the half-life in the terminal phase, which is a function of hybrid parameters including $PS_{net,\ eff}$ and PS_{bile}, was much lower in TR$^-$ compared to Wistar rats (27). Moreover, although the total amount of TC excreted into the bile was similar in TR$^-$ and Wistar rats, the biliary excretion rate in mutants was slower than that in normal rats (27). In the same manner, Takikawa *et al.* (3) demonstrated that the biliary excretion of intravenously infused TC in EHBR was significantly lower compared with that in SD rats. These results may be accounted for by the altered $PS_{net,\ eff}$ and PS_{bile} values in Mrp2-deficient rats.

As described in equation 5 and 6, $PS_{net,\ eff}$ is given as a hybrid parameters of Q, PS_{inf}, PS_{eff}, and PS_{bile}. To determine the intrinsic PS_{eff}, PS_{inf} was determined by the multiple indicator dilution method (Fig. 5). As shown in the Table I, PS_{inf} was comparable between SD rats and EHBR. This observation is consistent with the comparable expression level of Ntcp and Oatp-1 between SD rats and EHBR (Fig. 6). Moreover, the calculated PS_{eff} in EHBR was 2.3 times higher than

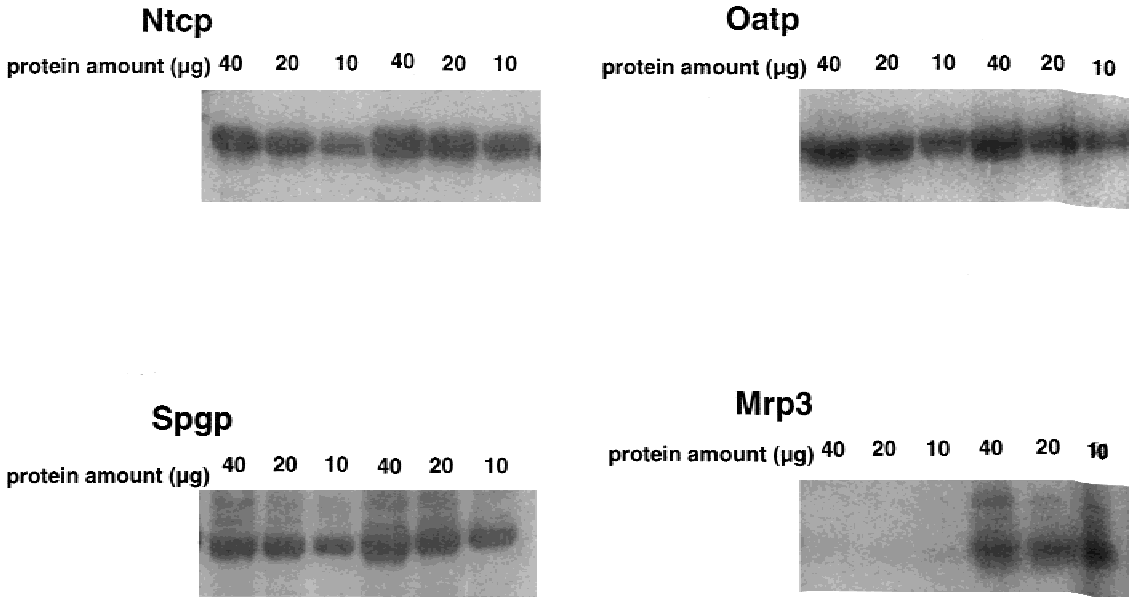

Fig. 6. Western blot analysis of rat Ntcp, Oatp-1, Spgp, and Mrp3 proteins in crude membranes isolated from SD rats and EHBR. Plasma membrane specimens (10, 20, and 40 μg) prepared from the liver form SD rats and EHBR were separated on 12.5% (Ntcp and Oatp-1) and 8.5 % (Spgp and Mrp3) polyacrylamide gel containing 0.1 % SDS. The proteins transferred to the polyvinylidene difluoride membrane by electroblotting were detected by polyclonal antibodies against Ntcp, Oatp-1, Spgp, and Mrp3.

that in SD rats, suggesting that elevated $PS_{net,\ eff}$ was predominantly associated with the increased sinusoidal efflux of [^{3}H]TC, rather than the decreased influx of [^{3}H]TC.

We demonstrated previously that expression of Mrp3 was increased under the cholestatic condition (e.g., bile duct ligation treated rats) and in Mrp2-deficient rats. Along with the animal models, enhanced expression of human Mrp3 on the basolateral membrane of hepatocyte was also observed in Dubin–Johnson syndrome subjects, in which function of Mrp2 is hereditary defective (20). Moreover, it was shown that rat Mrp3 transports several organic anions and bile acids (21,22). If we consider these results, it is possible that the increase in PS_{eff} in EHBR may be accounted for, at least partially, by the increased expression of Mrp3 in EHBR. Several pieces of previous observations are also consistent with this hypothesis. Previously, we found that the PS product for sinusoidal efflux of glucuronide conjugate of xenobiotics [e.g. E3040 glucuronide, a Mrp 3 substrate (21)] is higher in EHBR than that in SD rats (28). In contrast, no difference was observed between SD rats and EHBR in the sinusoidal efflux of E3040 sulfate, which is not significantly transported by Mrp3 (21,28). In addition, Xiong *et al.* (29) demonstrated much more efficient sinusoidal efflux of acetaminophen glucuronide in TR^- than that in Wistar rats. At the present moment, however, we cannot unequivocally conclude the increase in PS_{eff} of several organic anions in EHBR to the increased expression of Mrp3. Because Mrp3 is also induced in other cholestatic condition (e.g., bile duct treated rats) and accepts sulfated bile acids (such as taurolithocholate sulfate) and other glucuronide conjugates (21,22,28) [such as bilirubin monoglucuronide (30)], it is important to compare the hepatic disposition of these endogenous compounds between normal rats, Mrp2-deficient rats, and other cholestatic model rats in order to identify the role of Mrp3 under pathologic conditions. In addition, the utilization of specific inhibitor of Mrp3 in the perfused liver is required to quantify the role of Mrp3.

In conclusion, by comparing the disposition of TC between SD rats and EHBR, we were able to show that the PS product for TC across the sinusoidal membrane is increased in Mrp2-deficient rats. Along with the previous findings, it is possible that the increased expression of Mrp3 on the hepatic sinusoidal membrane may be responsible for the altered hepatic disposition of organic anions under pathologic conditions.

REFERENCES

1. H. Takikawa, H. Otsuka, T. Beppu, Y. Seyama, and T. Yamakawa. Serum concentrations of bile acid glucuronides in hepatobiliary diseases. *Digestion* **27:**189–195 (1983).
2. T. Kinugasa, K. Uchida, M. Kadowaki, H. Takase, Y. Nomura, and Y. Saito. Effect of bile duct ligation on bile acid metabolism in rats. *J. Lipid Res.* **22**:201–207 (1981).
3. H. Takikawa, N. Sano, T. Narita, Y. Uchida, M. Yamanaka, T. Horie, T. Mikami, and O. Tagaya. Biliary excretion of bile acid conjugates in a hyperbilirubinemic mutant Sprague-Dawley rat. *Hepatology* **14**:352–360 (1991).
4. F. Kuipers, M. Enserink, R. Havinga, A. B. van der Steen, M. J. Hardonk, J. Fevery, and R. J. Vonk. Separate transport systems for biliary secretion of sulfated and unsulfated bile acids in the rat. *J. Clin. Invest.* **81**:1593–1599 (1988).
5. R. P. Oude Elferink, D. K. Meijer, F. Kuipers, P. L. Jansen, A. K. Groen, and G. M. Groothuis. Hepatobiliary secretion of organic compounds; molecular mechanisms of membrane transport. *Biochim. Biophys. Acta.* **1241**:215–268 (1995).
6. J. König, A. T. Nies, Y. Cui, I. Leier, and D. Keppler. Conjugate export pumps of the multidrug resistance protein (MRP) family: Localization, substrate specificity, and MRP2-mediated drug resistance. *Biochim. Biophys. Acta.* **1461**:377–394 (1999).
7. H. Suzuki and Y. Sugiyama. Excretion of GSSG and glutathione conjugates mediated by MRP1 and cMOAT/MRP2. *Semin. Liver Dis.* **18**:359–376 (1998).
8. B. Hagenbuch, B. Stieger, M. Foguet, H. Lubbert, and P. J. Meier. Functional expression cloning and characterization of the hepatocyte Na^+/bile acid cotransport system. *Proc. Natl. Acad. Sci. USA* **88**:10629–10633 (1991).
9. B. Hagenbuch and P. J. Meier. Molecular cloning, chromosomal localization, and functional characterization of a human liver Na^+/bile acid cotransporter. *J. Clin. Invest.* **93**:1326–1331 (1994).
10. P. J. Meier, U. Eckhardt, A. Schroeder, B. Hagenbuch, and B. Stieger. Substrate specificity of sinusoidal bile acid and organic anion uptake systems in rat and human liver. *Hepatology* **26**: 1667–1677 (1997).
11. C. Reichel, B. Gao, J. Van Montfoort, V. Cattori, C. Rahner, B. Hagenbuch, B. Stieger, T. Kamisako, and P. J. Meier. Localization and function of the organic anion-transporting polypeptide Oatp2 in rat liver. *Gastroenterology* **117**:688–695 (1999).
12. J. König, Y. Cui, A. T. Nies, and D. Keppler. A novel human organic anion transporting polypeptide localized to the basolateral hepatocyte membrane. *Am. J. Physiol. Gastrointest. Liver Physiol.* **278**:G156–G164 (2000).
13. I. Tamai, J. Nezu, H. Uchino, Y. Sai, A. Oku, M. Shimane, and A. Tsuji. Molecular identification and characterization of novel members of the human organic anion transporter (OATP) family. *Biochem. Biophys. Res. Commun.* **273**:251–260 (2000).
14. H. Akita, H. Suzuki, K. Ito, S. Kinoshita, N. Sato, H. Takikawa, and Y. Sugiyama. Characterization of bile acid transport mediated by multidrug resistance associated protein 2 and bile salt export pump. *Biochim. Biophys. Acta.* **1511**:7–16 (2001).
15. T. Gerloff, B. Stieger, B. Hagenbuch, J. Madon, L. Landmann, J. Roth, A. F. Hofmann, and P. J. Meier. The sister of P-glycoprotein represents the canalicular bile salt export pump of mammalian liver. *J. Biol. Chem.* **273**:10046–10050 (1998).
16. B. Stieger, K. Fattinger, J. Madon, G. A. Kullak-Ublick, and P. J. Meier. Drug- and estrogen-induced cholestasis through inhibition of the hepatocellular bile salt export pump (Bsep) of rat liver. *Gastroenterology* **118**:422–430 (2000).
17. T. Hirohashi, H. Suzuki, K. Ito, K. Ogawa, K. Kume, T. Shimizu, and Y. Sugiyama. Hepatic expression of multidrug resistance-associated protein-like proteins maintained in eisai hyperbilirubinemic rats. *Mol. Pharmacol.* **53**:1068–1075 (1998).
18. K. Ogawa, H. Suzuki, T. Hirohashi, T. Ishikawa, P. J. Meier, K. Hirose, T. Akizawa, M. Yoshioka, and Y. Sugiyama. Characterization of inducible nature of MRP3 in rat liver. *Am. J. Physiol. Gastrointest. Liver Physiol.* **278**:G438–G446 (2000).
19. M. Kool, M. van der Linden, M. de Haas, G. L. Scheffer, J. M. de Vree, A. J. Smith, G. Jansen, G. J. Peters, N. Ponne, R. J. Scheper, R. P. Elferink, F. Baas, and P. Borst. MRP3, an organic anion transporter able to transport anti-cancer drugs. *Proc. Natl. Acad. Sci. USA* **96**:6914–6919 (1999).
20. J. König, D. Rost, Y. Cui, and D. Keppler. Characterization of the human multidrug resistance protein isoform MRP3 localized to the basolateral hepatocyte membrane. *J. Biol. Chem.* **274**: 15181–15185 (1999).
21. T. Hirohashi, H. Suzuki, and Y. Sugiyama. Characterization of the transport properties of cloned rat multidrug resistance-associated protein 3 (MRP3). *J. Biol. Chem.* **274**:15181–15185 (1999).
22. T. Hirohashi, H. Suzuki, H. Takikawa, and Y. Sugiyama. ATP-dependent transport of bile salts by rat multidrug resistance-associated protein 3 (Mrp3). *J. Biol. Chem.* **275**:2905–2910 (2000).
23. E. Jacquemin, B. Hagenbuch, B. Stieger, A. W. Wolkoff, and P. J. Meier. Expression cloning of a rat liver Na(+)-independent organic anion transporter. *Proc. Natl. Acad. Sci. USA* **91**:133–137 (1994).
24. B. Stieger, B. Hagenbuch, L. Landmann, M. Hochli, A. Schroeder, and P. J. Meier. In situ localization of the hepatocytic Na+/Taurocholate cotransporting polypeptide in rat liver. *Gastroenterology* **107**:1781–1787 (1994).
25. H. Sato, Y. Sugiyama, Y. Sawada, T. Iga, S. Sakamoto, T. Fuwa,

and M. Hanano. Dynamic determination of kinetic parameters for the interaction between polypeptide hormones and cell-surface receptors in the perfused rat liver by the multiple-indicator dilution method. *Proc. Natl. Acad. Sci. USA* **85**:8355–8359 (1988).
26. S. Miyauchi, Y. Sawada, T. Iga, M. Hanano, and Y. Sugiyama. The influence of glucagon on the hepatic transport of taurocholate in isolated perfused rat liver: Kinetic analysis by the multiple indicator dilution technique. *Biol. Pharm. Bull.* **16**:791–795 (1993).
27. P. L. Jansen, G. M. Groothuis, W. H. Peters, and D. F. Meijer. Selective hepatobiliary transport defect for organic anions and neutral steroids in mutant rats with hereditary-conjugated hyperbilirubinemia. *Hepatology* **7**:71–76 (1987).
28. O. Takenaka, T. Horie, K. Kobayashi, H. Suzuki, and Y. Sugiyama. Kinetic analysis of hepatobiliary transport for conjugated metabolites in the perfused liver of mutant rats (EHBR) with hereditary conjugated hyperbilirubinemia. *Pharm. Res.* **12**:1746–1755 (1995).
29. H. Xiong, K. C. Turner, E. S. Ward, P. L. Jansen, and K. L. Brouwer. Altered hepatobiliary disposition of acetaminophen glucuronide in isolated perfused livers from multidrug resistance-assisted protein 2-deficient TR^- rats. *J. Pharmacol. Exp. Ther.* **295**:512–518 (2001).
30. D. Keppler, T. Kamisako, I. Leier, Y. Cui, A. T. Nies, H. Tsujii, and J. König. Localization, substrate specificity, and drug resistance conferred by conjugate export pumps of the MRP family. *Adv. Enzyme Regul.* **40**:339–349 (2000).